Blue-Light-Emitting and Anodically Electrochromic Materials of New Wholly Aromatic Polyamides Derived from the High-Efficiency Chromophore 4,4′-Dicarboxy-4″-methyltriphenylamine

GUEY-SHENG LIOU, NAN-KUN HUANG, YI-LUNG YANG

Department of Applied Chemistry, National Chi Nan University, 1 University Road, Nantou Hsien 545, Taiwan, Republic of China

ABSTRACT: A series of organosoluble, aromatic polyamides were synthesized from a 4-methyl-substituted, triphenylamine-containing, aromatic diacid monomer, 4,4′-dicarboxy-4″-methyltriphenylamine, which is a blue-light (454-nm) emitter with a fluorescence quantum efficiency of 46%. These triphenylamine-based, high-performance polymers had strong fluorescence emissions in the blue region with high quantum yields up to 64% and one reversible oxidation redox couple around 1.20 V versus Ag/AgCl in acetonitrile solutions. They exhibited good thermal stability, with 10% weight loss temperatures above 480 °C under a nitrogen atmosphere and with relatively high glass-transition temperatures (252–309 °C). All the polyamides revealed excellent stability of electrochromic characteristics, changing color from the original pale yellow to blue. © 2006 Wiley Periodicals, Inc. J Polym Sci Part A: Polym Chem 44: 4095–4107, 2006

Keywords: electrochemistry; fluorescence; functionalization of polymers; high performance polymers; polyamides; polycondensation

INTRODUCTION

Triarylamines have attracted considerable interest as hole-transport materials for use in multilayer organic electroluminescence (EL) devices because of their relatively high mobilities and their low ionization potentials.[1–4] The feasibility of using spin-coating and ink-jet printing processes for large-area EL devices and the possibility of various chemical modifications (to improve emission efficiencies and allow patterning) make polymeric materials containing triarylamine units very attractive.[5–9] To enhance the hole-injection ability of polymeric emissive materials such as poly(1,4-phenylenevinylene)s (PPV) and polyfluorenes (PFs), there have been several reports on PPV and PF derivatives involving hole-transporting units such as triarylamine or carbazole groups in the emissive π-conjugated core/main chains,[10–17] grafting them as side chains in a polymer,[18–23] and attaching them onto the polymer chain ends or the outer surface of dendritic wedges.[24,25] However, the solubility of many highly conjugated polymers is low, particularly for blue-emitting species. These targeted blue-emitting polymers therefore often bear large alkyl, alkoxy, or aryloxy groups to improve their solubility, which lower their glass-transition temperatures (T_g's) and thermal stability.

To obtain high-T_g, hole-transporting polymers, many investigators have prepared polymers containing triphenylamine units in the main

chain.[26–30] Such electroactive sites can be provided by triphenylamines, which are electron-rich aromatics and are readily oxidized to form cationic radical conducting salts. Ogino and coworkers[26,27] successfully prepared triphenylamine-containing polymers with hole-transporting ability. Kakimoto and coworkers[28–30] reported that the charge injection and EL efficiency were improved remarkably by the incorporation of a hole-transporting polyimide containing triphenylamine moieties in the backbone. Recently, we reported the synthesis of soluble, aromatic polyamides and polyimides bearing triphenylamine units in the main chain based on N,N-bis(4-aminophenyl)-N′,N′-diphenyl-1,4-phenylenediamine,[31,32] N,N-bis(4-carboxyphenyl)-N′,N′-diphenyl-1,4-phenylenediamine,[33] and 2,4-diaminotriphenylamine,[34] respectively. Because of the incorporation of bulky, three-dimensional triphenylamine units along the polymer backbone, all the polymers were amorphous, had good solubility in many aprotic solvents, and exhibited excellent thin-film-forming capability. In this article, we therefore report a novel class of triphenylamine-containing polyamides derived from a dicarboxylic acid, 4,4′-dicarboxy-4″-methyltriphenylamine (2), which is a blue-light (454-nm) emitter with a fluorescence quantum efficiency of 46%, and various aromatic diamines. The general properties of these polymers, such as the solubility, crystallinity, and thermal and mechanical properties, are reported. The electrochemical, electrochromic, and photoluminescent properties of these polymers, which were prepared by the casting of solutions onto indium tin oxide (ITO) coated glass substrates, are also described herein and are compared with those of structurally related polymers from 4,4′-dicarboxytriphenylamine.[35]

EXPERIMENTAL

Materials

4-Methylaniline (Lancaster), sodium hydride (95%; dry; Aldrich), 4-fluorobenzonitrile (TCI), potassium hydroxide (Tedia), N,N-dimethylacetamide (DMAc; Tedia), N,N-dimethylformamide (DMF; Acros), dimethyl sulfoxide (DMSO), N-methyl-2-pyrrolidinone (NMP; Tedia), pyridine (Py; Tedia), and triphenyl phosphite (TPP; Acros) were used without further purification. Commercially available aromatic diamines such as p-phenylenediamine (2b; TCI), m-phenylenediamine (TCI), and 4,4′-oxydianiline (TCI) were used as received. Anhydrous calcium chloride (CaCl₂) was dried in vacuo at 180 °C for 3 h. Tetrabutylammonium perchlorate (TBAP) was obtained from Acros and recrystallized twice from ethyl acetate and then was dried in vacuo before use. All other reagents were used as received from commercial sources.

Preparation of 4,4′-Dicyano-4″-methyltriphenylamine (1)

A mixture of 4.80 g (0.20 mol) of sodium hydride and 180 mL of DMF was stirred at room temperature. To the mixture, 8.60 g (0.08 mol) of 4-methylaniline and 19.38 g (0.16 mol) of 4-fluorobenzonitrile were added in sequence. The mixture was heated with stirring at 150 °C for 15 h under nitrogen and then precipitated into 400 mL of cold water. The products was filtered and recrystallized from acetonitrile and was dried to give a yellowish solid (8.38 g, yield = 45%).

mp: 219–222 °C (lit.[36] 215–216 °C) by differential scanning calorimetry (DSC) at 10 °C/min. IR (KBr): 2218 cm⁻¹ (C≡N). ¹H NMR (500 MHz, CDCl₃, δ, ppm): 2.38 (S, 1H, CH₃), 7.07 (d, 2H, H_c), 7.11 (d, 4H, H_b), 7.20 (d, 2H, H_d), 7.50 (d, 4H, H_a). ¹³C NMR (500 MHz, CDCl₃, δ, ppm): 21.0 (CH₃), 105.3 (C¹), 118.9 (CN), 122.5 (C³), 127.0 (C⁶), 131.0 (C⁷), 133.9 (C²), 137.0 (C⁸), 142.2 (C⁵), 150.0 (C⁴). ELEM. ANAL. Calcd. for C₂₁H₁₅N₃ (309.13): C, 81.53%; H, 4.89%; N, 13.58%. Found: C, 81.47%; H, 4.92%; N, 13.53%.
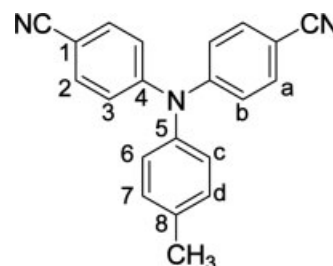
Preparation of 4,4′-Dicarboxy-4″-methyltriphenylamine (2)

A mixture of 21.88 g of potassium hydroxide and 5.50 g of dicyano compound 1 in 20 mL of ethanol and 30 mL of distilled water was stirred at approximately 100 °C until no further ammonia was generated. The time taken to reach this stage was about 4–5 days. The solution was cooled, and the pH value was adjusted by dilute hydrochloric acid to nearly 3. The yellowish precipitate was collected by filtration and washed thoroughly with water. Recrystallization from acetic acid and then drying at 150 °C in vacuo gave 4.23 g (yield = 69%) of the diacid.

**Table 1.** Inherent Viscosity (η_{inh}) and Elemental Analysis of the Polyamides

Poly(amine amide)		Elemental Analysis (%)				
Code	η_{inh} (dL/g)[a]	Formula (Molecular Weight)		C	H	N
3a	0.51	$(C_{45}H_{33}N_3O_2)_n$	Calcd.	83.44	5.13	6.49
		$[(647.76)_n]$	Found	82.36	5.20	6.35
3b	1.14	$(C_{27}H_{21}N_3O_2)_n$	Calcd.	77.31	5.05	10.02
		$[(419.47)_n]$	Found	76.62	5.15	9.89
3c	0.90	$(C_{27}H_{21}N_3O_2)_n$	Calcd.	77.31	5.05	10.02
		$[(419.47)_n]$	Found	76.94	5.12	9.96
3d	0.90	$(C_{33}H_{25}N_3O_3)_n$	Calcd.	77.48	4.93	8.21
		$[(511.57)_n]$	Found	76.60	5.01	8.12
3e	0.54	$(C_{51}H_{39}N_5O_2)_n$	Calcd.	81.25	5.21	9.21
		$[(753.89)_n]$	Found	80.93	5.22	9.16
3f	0.42	$(C_{47}H_{17}F_6N_3O_4)_n$	Calcd.	69.20	3.83	5.15
		$[(815.22)_n]$	Found	68.79	3.89	4.99
3g	0.52	$(C_{45}H_{33}N_3O_4)_n$	Calcd.	79.51	4.89	6.18
		$[(679.25)_n]$	Found	79.14	4.97	6.09

[a] Measured at a polymer concentration of 0.5 g/dL in DMAc at 30 °C.

mp: 278–281 °C (lit.[32] 188–190 °C) by DSC at 10 °C/min. IR (KBr): 1684 (C=O), 2700–3400 cm^{-1}(O—H). ^{1}H NMR (500 MHz, DMSO-d_6, δ, ppm): 2.38 (S, 1H, CH$_3$), 7.05–7.01 (m, 6H, H$_b$ + H$_c$), 7.23 (d, 2H, H$_d$), 7.84 (d, 2H, H$_a$), 12.65 (s, 2H, —COOH). ^{13}C NMR (500 Hz, DMSO-d_6, δ, ppm): 21.0 (CH$_3$), 122.0 (C^3), 124.5 (C^1), 127.2 (C^6), 131.0 (C^7), 130.2 (C^2), 135.6 (C^8), 130.1 (C^5), 150.4 (C^4), 167 (C=O). ELEM. ANAL. Calcd. for C$_{21}$H$_{17}$NO$_4$ (347.12): C, 72.61%; H, 4.96%; N, 4.03%. Found: C, 72.49%; H, 5.01%; N, 4.06%.
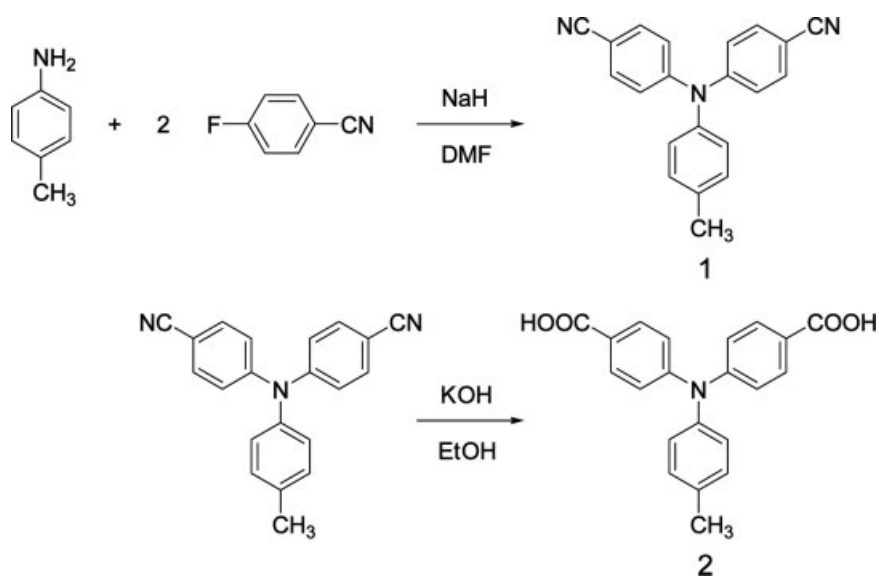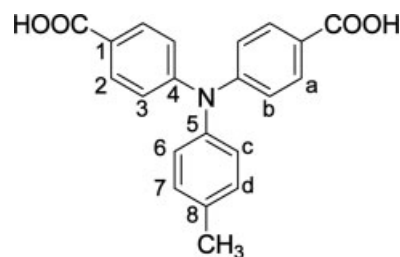
Scheme 1. Monomer synthesis.
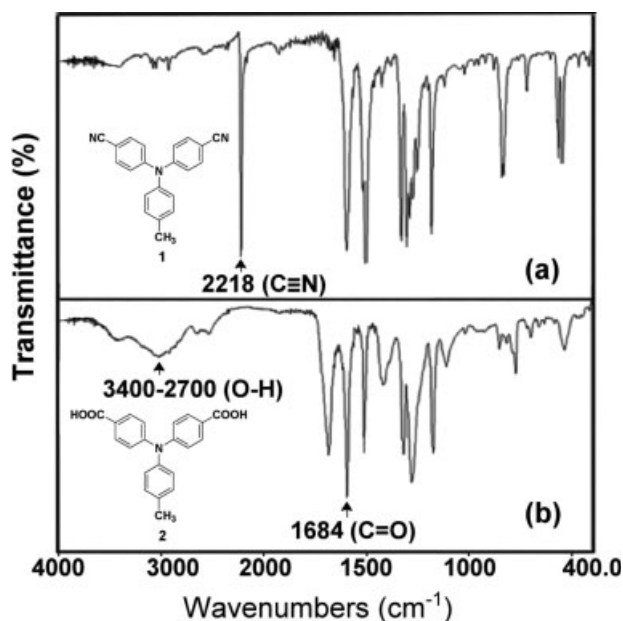
Figure 1. IR spectra of (a) dinitrile compound **1** and (b) dicarboxylic acid compound **2**.

Preparation of the Polyamides via the Phosphorylation Reaction

The synthesis of polyamide **3b** is used as an example to illustrate the general synthetic route. A typical procedure was as follows. A mixture of 0.43 g (1.25 mmol) of **2**, 0.14 g (1.25 mmol) of **2b**, 0.15 g of $CaCl_2$, 0.9 mL of TPP, 0.6 mL of Py, and 2.5 mL of NMP was heated with stirring at 105 °C for 3 h. The polymer solution was poured slowly into 300 mL of stirring methanol; this gave rise to a stringy, fiberlike precipitate that was collected by filtration, washed thoroughly with hot water and methanol, and dried *in vacuo* at 150 °C for 15 h *in vacuo*. Precipitations from DMAc into

methanol were carried out twice for further purification. The inherent viscosity of the obtained polyamide was 1.14 dL/g (measured at a concentration of 0.5 g/dL in NMP at 30 °C). The IR spectrum of **3b** (film) exhibited characteristic amide absorption bands at 3301 (N—H stretching) and 1645 cm^{-1} (amide carbonyl).

ELEM. ANAL. Calcd. for $(C_{27}H_{21}N_3O_2)_n$ [$(419.18)_n$]: C, 77.31%; H, 5.05%; N, 10.02%. Found: C, 76.62%; H, 5.15%; N, 9.89% (Table 1).

Measurements

IR spectra were recorded on a PerkinElmer RXI Fourier transform infrared (FTIR) spectrometer. ^{1}H and ^{13}C NMR spectra were measured on a Bruker Avance 500-MHz FT-NMR system. Elemental analyses were run on an Elementar Vario EL-III. The inherent viscosities were determined at a 0.5 g/dL concentration with an Tamson TV-2000 viscometer at 30 °C. Wide-angle X-ray diffraction (WAXD) measurements of the polymer films were performed at room temperature (ca. 25 °C) on a Shimadzu XRD-7000 X-ray diffractometer (40 kV and 20 mA) with a graphite monochromator with nickel-filtered Cu Kα radiation. Ultraviolet–visible (UV–vis) spectra of the polymer films were recorded on a Varian Cary 50 probe spectrometer. An Instron model 4400R universal tester with a load cell of 5 kg was used to study the stress–strain behavior of the samples. A gauge length of 2 cm and a crosshead speed of 5 mm/min were used for this study. The measurements were performed at room temperature with film specimens (0.5 cm wide and 6 cm long), and an average of at least three replicates was used. Thermogravimetric analysis (TGA) was conducted with a PerkinElmer Pyris 1 thermogravimetric analyzer. The experiments were carried
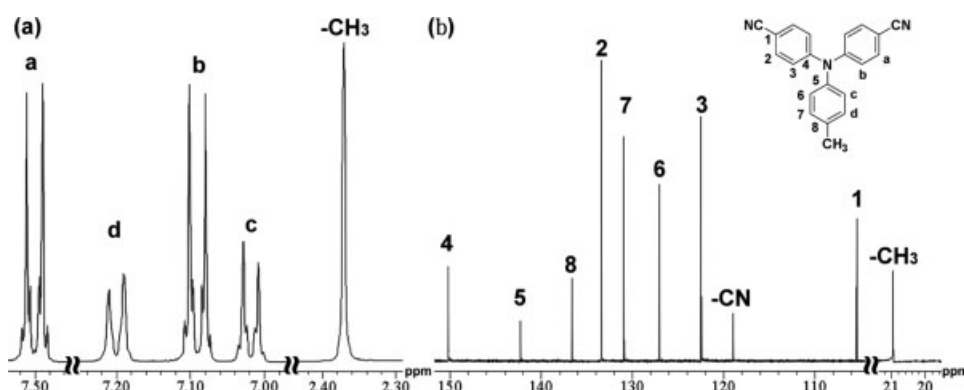

Figure 2. (a) ^{1}H NMR and (b) ^{13}C NMR spectra of compound **1** in $CDCl_3$.
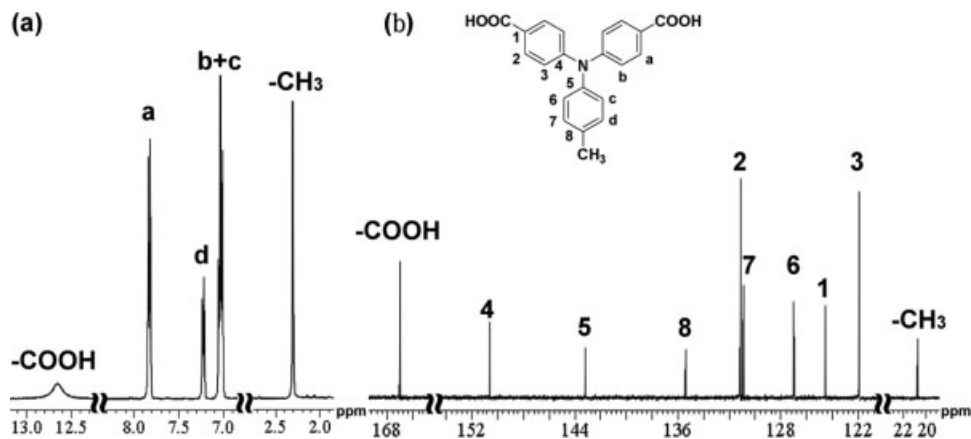
Figure 3. (a) ^{1}H NMR and (b) ^{13}C NMR spectra of compound **2** in DMSO-d_6.

out on approximately 6–8-mg film samples heated in flowing nitrogen or air (flow rate = 40 cm^3/min) at a heating rate of 20 °C/min. DSC analyses were performed on a PerkinElmer Pyris 1 DSC instrument at a scanning rate of 20 °C/min in flowing nitrogen (20 cm^3/min). Electrochemistry was performed with a CHI 611B electrochemical analyzer. Voltammograms are presented with the

positive potential pointing to the left and with increasing anodic currents pointing downward. Cyclic voltammetry was performed with the use of a three-electrode cell, in which ITO (polymer film area $\sim$ 0.7 cm $\times$ 0.5 cm) was used as a working electrode. A platinum wire was used as an auxiliary electrode. All cell potentials were taken with the use of a homemade Ag/AgCl or KCl (sat-
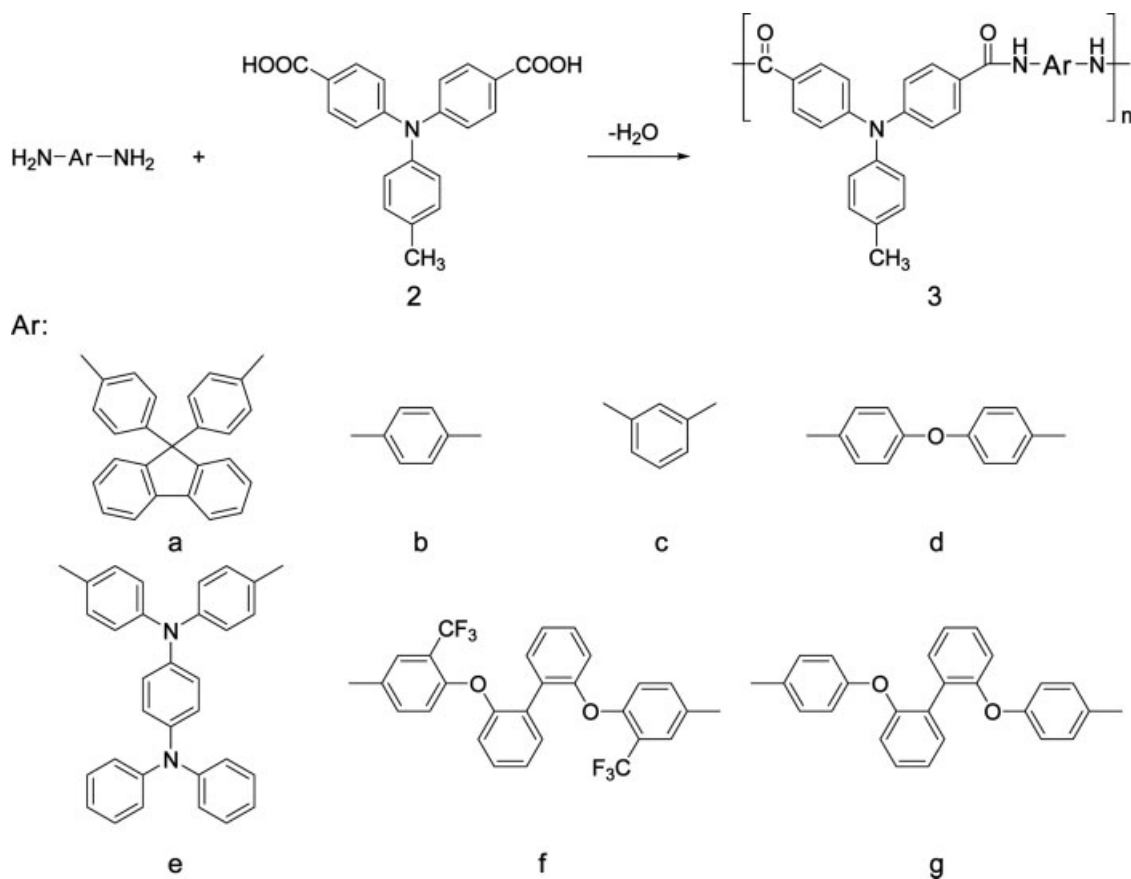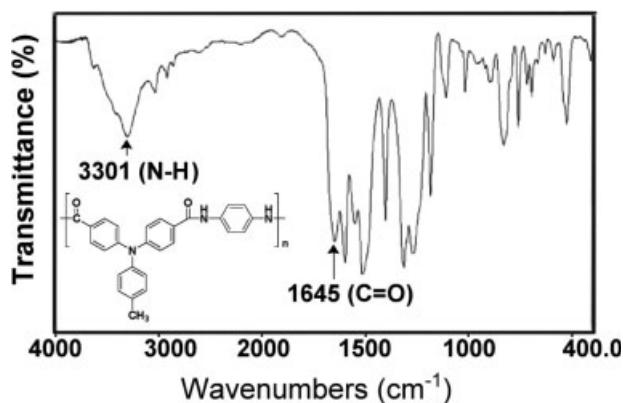

Scheme 2. Polymer synthesis.

Figure 4. Film FTIR spectra of polyamide **3b**.

urated) reference electrode. The spectroelectrochemical cell was composed of a 1-cm cuvette, ITO as a working electrode, a platinum wire as an auxiliary electrode, and a Ag/AgCl KCl (saturated) reference electrode. Absorption spectra were measured with an HP 8453 UV–vis spectrophotometer. Photoluminescence spectra were measured with a Jasco FP-6300 spectrofluorometer.

RESULTS AND DISCUSSION

Monomer Synthesis

An aromatic dicarboxylic acid with a bulky, methyl-substituted triphenylamine group (**2**) was synthesized by the amination reaction of 4-methylaniline with 4-fluorobenzonitrile, followed by the alkaline hydrolysis of the intermediate dinitrile compound, according to the synthetic routes outlined in Scheme 1. Elemental analysis and IR, ^{1}H NMR, and ^{13}C NMR spectroscopy techniques were used to identify the structures of the intermediate dinitrile compound (**1**) and the dicar-

boxylic acid monomer (**2**). The IR spectra of **1** gave a characteristic cyano group band at 2218 cm^{-1} (stretching). After hydrolysis, the characteristic absorption of the cyano group disappeared, and the carboxylic acid group showed a typical carbonyl absorption band at 1684 cm^{-1} (C=O stretching) together with the appearance of broad bands around 2700–3400 cm^{-1} (O—H stretching; Fig. 1). The structures of compounds **1** and **2** were also confirmed by high-resolution NMR spectra (Figs. 2 and 3). The ^{13}C NMR spectra confirmed that the cyano groups were completely converted into the carboxylic acid groups by the disappearance of the resonance peak for the cyano carbon at 118.9 ppm and by the appearance of the carbonyl peak at 167 ppm. Other important evidence of this change was the shifting of the carbon resonance signals of C^1 adjacent to the cyano or carboxyl group. The C^1 of dinitrile **1** resonated at a higher field (105.3 ppm) than the other aromatic carbons because of the anisotropic shielding by the π electrons of C≡N. After hydrolysis, the resonance peak of C^1 shifted to a lower field (124.5 ppm) because of the lack of an anisotropic field.

Polymer Synthesis

A series of new aromatic polyamides with methyl-substituted triphenylamine units were prepared from the dicarboxylic acid (**2**) and various aromatic diamines by the direct polycondensation reaction with TPP and Py as condensing agents (Scheme 2). All the polymerizations proceeded homogeneously throughout the reaction and afforded clear, highly viscous polymer solutions. All the polymers precipitated in a fiberlike form when the resulting polymer solutions were slowly poured into methanol. These polyamides were obtained in almost quantitative yields with inher-
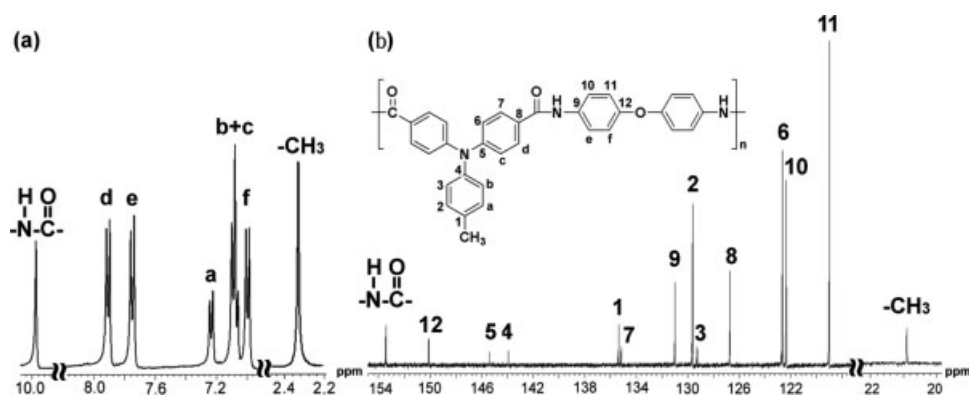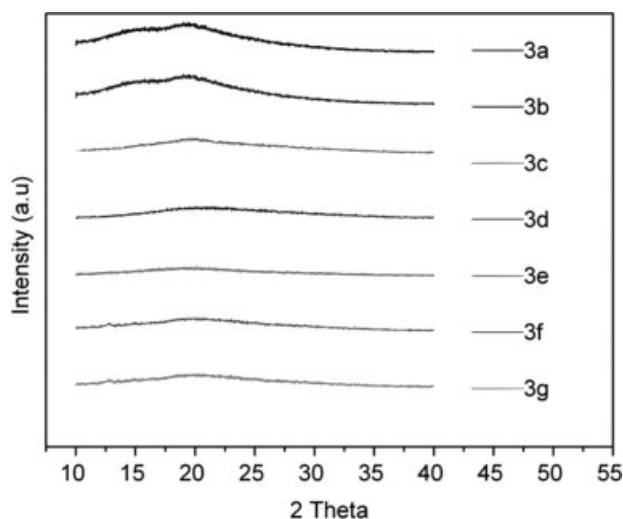

Figure 5. (a) ^{1}H NMR and (b) ^{13}C NMR spectra of polyamide **3d** in DMSO-d_6.

Figure 6. WAXD patterns of the polyamide films.

ent viscosity values in the range of 0.42–1.14 dL/g (Table 1), and the formation of polyamides was confirmed by elemental analysis and IR, ^{1}H NMR, and ^{13}C NMR spectroscopy. The elemental analysis values of these polymers are listed in Table 1. Figure 4 shows a typical set of IR spectra for polyamide **3b** with the characteristic absorption bands of the amide group around 3301 (N—H stretching) and 1645 cm^{-1} (amide carbonyl). Figure 5 shows a typical set of ^{1}H and ^{13}C NMR spectra of polyamide **3d** in DMSO-d_6; all the peaks have been readily assigned to the hydrogen and carbon atoms of the recurring unit.

Polymer Properties

Basic Characterization

From the typical diffraction patterns shown in Figure 6, the X-ray diffraction studies of the polyamides indicated that all the polymers were essentially amorphous. The solubility behavior of polyamides was tested qualitatively, and the results are presented in Table 2. All the polyamides were highly soluble in polar solvents such as NMP, and the enhanced solubility can be attributed to the introduction of a methyl-substituted triphenylamine group into the repeat unit. Thus, the excellent solubility makes these polymers potential candidates for practical applications by spin- or dip-coating processes. All the aromatic polyamides could afford transparent and flexible films. These films were subjected to tensile testing, and the results are given in Table 3. The tensile strengths, elongations to break, and initial moduli of these films were in the ranges of 56–86 MPa, 5–56%, and 1.9–2.4 GPa, respectively. The thermal properties of the polyamides were investigated with TGA and DSC. The results are summarized in Table 4. Typical TGA curves of a representative polyamide (**3b**) in both air and nitrogen atmospheres are shown in Figure 7; all the polyamides exhibited good thermal stability with insignificant weight loss up to 400 °C in nitrogen. The 10% weight loss temperatures of the polyamides in nitrogen and air were recorded in the ranges of 482–580 and 476–568 °C, respectively. The amount of carbonized residue (char yield) of these polymers in a nitrogen atmosphere was more than 53% at 800 °C. The high char yields of these polymers could be ascribed to their high aromatic content. The T_g's of all the polymers could be easily measured with the DSC thermograms; they were observed in the range of 252–309 °C. All the polymers indicated no clear melting endotherms up to the decomposition temperatures on the DSC scans.

Table 2. Solubility of the Polyamides

Polymer	Solvent[a]						
	NMP	DMAc	DMF	DMSO	*m*-Cresol	Tetrahydrofuran	CHCl$_3$
3a	+	+	+	−	+h	−	−
3b	+	+	+	−	+h	−	−
3c	+	+h	+h	−	−	−	−
3d	+	+	+	+	+h	−	−
3e	+	+	+	+h	+h	−	−
3f	+	+	+	+	+h	+	−
3g	+	+	+	+	+h	+h	−

[a] + = soluble at room temperature; +h = soluble on heating; − = insoluble even on heating.

Table 3. Mechanical Properties of the Polyamide Films

Polymer	Tensile Strength (MPa)	Elongation at Break (%)	Initial Modulus (GPa)
3a	59	5	1.9
3b	62	43	1.9
3c	74	8	2.3
3d	68	56	2.0
3e	56	20	1.9
3g	86	5	2.4

Optical and Electrochemical Properties

The optical and electrochemical properties of the polyamides were investigated with cyclic voltammetry and UV–vis and photoluminescence spectroscopy. The results are summarized in Table 5. These polymers exhibited strong UV–vis absorption bands at 352–370 nm in NMP solutions, which were assignable to the π–π* transition resulting from the conjugation between the aromatic rings and nitrogen atoms. The fluorescence spectra of the polyamides in NMP solutions exhibited emission maxima at 439–535 nm. The fluorescence quantum yield (Φ_f) of **3f** (0.64) measured in NMP was the highest among the series of polymers and was much higher than that of structurally similar **3g** (0.20). This may have been the result of the presence of bulky, electron-withdrawing trifluoromethyl (—CF$_3$) substitu-

Table 4. Thermal Properties of the Aromatic Polyamides

Polymer	T_g (°C)[a]	T_d at 5% Weight Loss (°C)[b] N$_2$	T_d at 5% Weight Loss (°C)[b] Air	T_d at 10% Weight Loss (°C)[b] N$_2$	T_d at 10% Weight Loss (°C)[b] Air	Char Yield (wt %)[c]
3a	—	507	501	580	557	76
3b	309	456	449	490	502	66
3c	274	455	468	507	512	65
3d	271	457	473	489	521	60
3e	288	504	510	559	568	70
3f	267	437	432	482	476	64
3g	252	469	474	510	521	54

[a] Midpoint temperature of the baseline shift on the second DSC heating trace (rate = 20 °C/min) of the sample after quenching from 400 °C.
[b] Decomposition temperature recorded via TGA at a heating rate of 20 °C/min and a gas flow rate of 30 cm^3/min.
[c] Residual weight percentage at 800 °C in nitrogen.
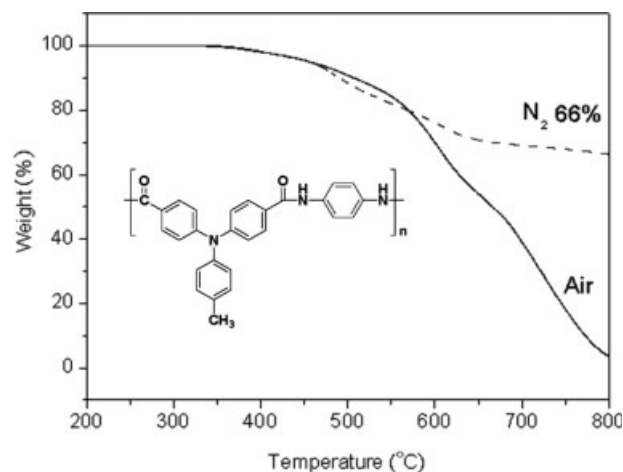
Figure 7. TGA thermograms of polyamide **3b** at a scanning rate of 20 °C/min.

ents in **3f**, which effectively restricted intramolecular and intermolecular charge-transfer (CT) interactions. On the contrary, polymer **3e** exhibited significantly less detectable fluorescence (Φ_f = $\sim 10^{-3}$) than the other polymers. The weak fluorescence of **3e** might be attributed to the introduction of a higher highest occupied molecular orbital (HOMO) energy level and an electron-donating diamine structure, which resulted in nonradiative decay by the formation of a CT or photoinduced electron-transfer effect between the diacid and diamine moieties. The solid-state emission spectra were similar to those recorded from the NMP solution. Although the solid-state emission of some of the polyamides was slightly red-shifted from the corresponding solution emission, the emission remained in the blue region. The photoluminescence images of the polymer solution and thin film of **3f** under UV irradiation are also shown in Figure 8, and both of them showed strong fluorescent blue light. The UV–vis transmittance spectra of the polyamide films and the cutoff wavelengths (absorption edge) in the range of 408–448 nm from the UV–vis spectra are also indicated in Figure 9. The electrochemical redox behavior was investigated by cyclic voltammetry conducted for the cast film on an ITO-coated glass substrate as a working electrode in dry acetonitrile (CH$_3$CN) containing 0.1 M TBAP as an electrolyte under a nitrogen atmosphere. The typical cyclic voltammograms for polyamides **3c** and **3e** are shown in Figure 10. There are three reversible oxidation redox couples at $E_{1/2}$ (average potential of the redox couple peaks) values of 0.60, 0.98, and 1.28 V for polyamide **3e** and one

Table 5. Optical and Electrochemical Properties for the Aromatic Polyamides

Index	Film Color	λ_0 (nm)[b]	$\lambda_{abs, max}$ (nm)[c]	$\lambda_{abs, onset}$ (nm)[c]	$\lambda_{PL, max}$ (nm)[d]	Oxidation (V) (vs. Ag / AgCl)			HOMO–LUMO Gap (eV)[f]	HOMO (eV)[g]	LUMO (eV)[h]	Φ_{PL} (%)[i]
						First	Second	Third				
3a		413	360 (353)	398 (403)	439 (450)	1.17	—	—	3.08	5.53	2.45	30
3b		424	370 (382)	396 (422)	443 (459)	1.16	—	—	2.94	5.52	2.58	1.2
3c		408	361 (384)	396 (421)	439 (456)	1.20	—	—	2.95	5.56	2.61	30
3c′		429	357 (361)	397 (401)	436 (448)	(1.30)[e]	—	—	3.09	5.66	2.57	13
3c″	—[a]	—	352 (357)	403 (406)	501 (498)	0.78	1.14	—	2.98	5.14	2.16	1.7
3d		416	360 (363)	395 (426)	439 (452)	1.20	—	—	2.91	5.56	2.65	8.5
3e		448	367 (361)	409 (424)	535 (525)	0.60	0.98	1.28	2.92	4.96	2.04	0.10
3f		410	366 (360)	399 (411)	453 (452)	1.20	—	—	3.02	5.57	2.55	64
3g		418	359 (361)	391 (405)	439 (451)	1.18	—	—	3.06	5.54	2.48	20

[a] The polymer was too brittle.
[b] Cutoff wavelength from the transmission UV–vis absorption spectra of the polymer films (50–80 μm).
[c] UV–vis absorption measurements in NMP (1×10^{-5} M) at room temperature (the values in parentheses are for the polymer thin films).
[d] Photoluminescence spectroscopy measurements in NMP (1×10^{-5} M) at room temperature (the values in parentheses are for the polymer thin films).
[e] Irreversible peak potential.
[f] The data were calculated for the thin film with the following equation: gap = $1240/\lambda_{onset}$.
[g] The HOMO energy levels were calculated from cyclic voltammetry and were referenced to ferrocene (4.8 eV).
[h] LUMO = HOMO − gap.
[i] Photoluminescence quantum yield measured with quinine sulfate (dissolved in 1 N aqueous H_2SO_4 with a concentration of 10^{-5} M, assuming $\Phi_{PL} = 0.55$) as a standard at 25 °C.[37,38]
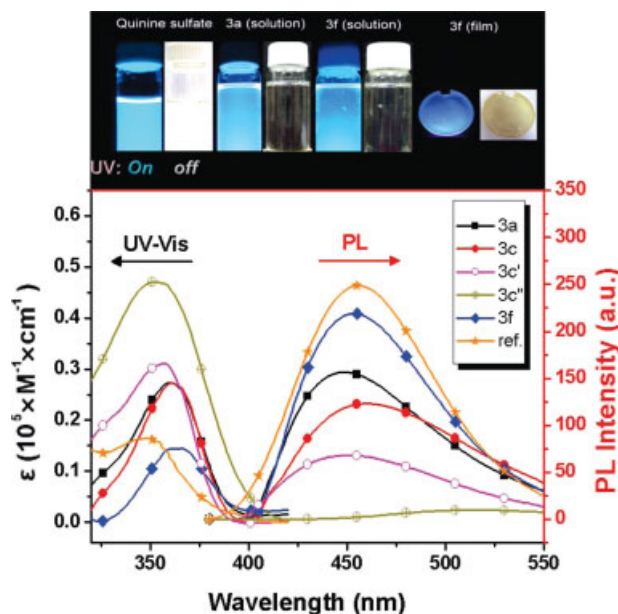
Figure 8. Molar absorptivity (ε) and photoluminescence (PL) of (★) quinine sulfate (ca. 1×10^{-5} M) in 1 N H_2SO_4 and polyamides (■) **3a**, (●) **3c**, (○) **3c′**, (⊕) **3c″**, and (◆) **3f** (ca. 1×10^{-5} M) in NMP solutions.

reversible oxidation redox couple at $E_{1/2} = 1.20$ V for polyamide **3c** in the oxidative scan. Because of the electrochemical stability of the films and good adhesion between the polymer and ITO substrate, polyamide **3e** 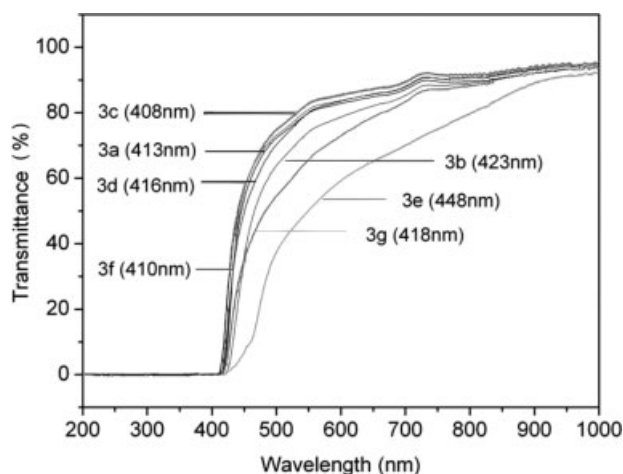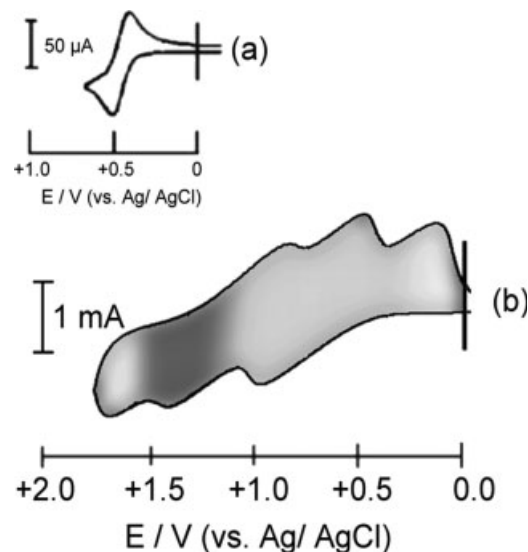exhibited excellent reversibility of electrochromic characteristics in 10 continuous cyclic scans between 0.0 and 1.40 V, changing color from the original pale yellow to green and then to blue at electrode potentials ranging from 0.70 to 1.40 V. The energy levels of the HOMO

**Figure 9.** Transmission UV–vis absorption spectra of some polyamide films (50–80 μm).

Figure 10. Cyclic voltammograms of (a) ferrocene and (b) a polyamide **3e** film on an ITO-coated glass substrate in CH_3CN containing 0.1 M TBAP (scanning rate = 0.1 V/s).

and lowest unoccupied molecular orbital (LUMO) of the investigated polyamides could be determined from the oxidation half-wave potentials and the onset absorption wavelength, and the results are listed in Table 5. For example, the oxidation half-wave potential for polyamide **3c** was determined to be 1.20 V versus Ag/AgCl. The external ferrocene/ferrocenium (Fc/Fc$^+$) redox standard potential $(E)_{1/2}$ was 0.44 V versus Ag/AgCl in CH_3CN. Assuming that the HOMO value for the Fc/Fc$^+$ standard was 4.80 eV with respect to the zero vacuum level, we evaluated the HOMO energy level for polyamide **3c** to be 5.56 eV.

Electrochromic Characteristics

The typical electrochromic absorption spectra of polyamides **3c** and **3e** are shown in Figures 11–14. When the applied potentials increased positively from 0.0 to 0.70, 1.10, and 1.40 V, the peak of the absorbance at 369 nm, characteristic for polyamide **3e**, decreased gradually, whereas one new band grew up at 1003 nm because of the first electron oxidation. When the potentials were adjusted to more positive values corresponding to the second and third electron oxidation, the new spectral change was assigned in Figures 12–14, and the film of **3e** changed from pale green to deep green and then to blue. The color switching times were estimated by the application of a potential step, and the absorbance profiles are shown in Figure 15. The switching time was
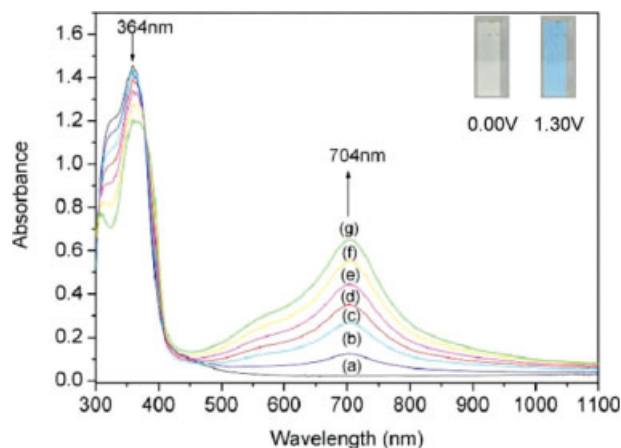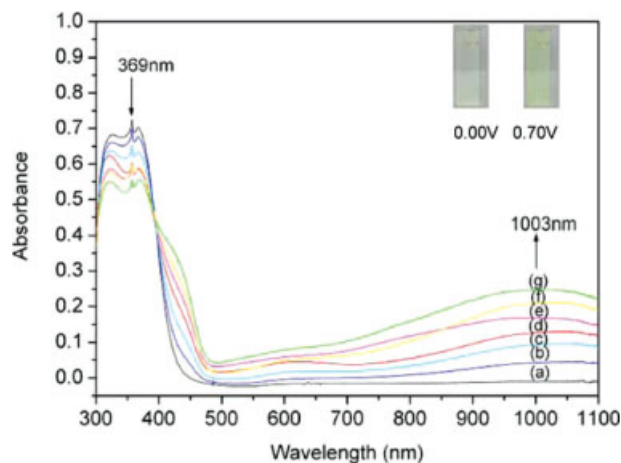
Figure 11. Electrochromic behavior of a polyamide **3c** thin film (in CH$_3$CN with 0.1 M TBAP as the supporting electrolyte) at (a) 0.00, (b) 1.15, (c) 1.18, (d) 1.21, (e) 1.24, (f) 1.27, and (g) 1.30 V.

defined as the time required to reach 90% of the full change in the absorbance after the application of the potential. A thin film of polyamide **3e** required 3 s at 0.70 V for switching the absorbance at 1003 nm and 2 s for bleaching. The time was about 2 s for switching the coloration at 735 nm and 1 s for bleaching and 3 s for coloration at 731 nm and 2 s for bleaching when the potential was set at 1.10 and 1.40 V, respectively.
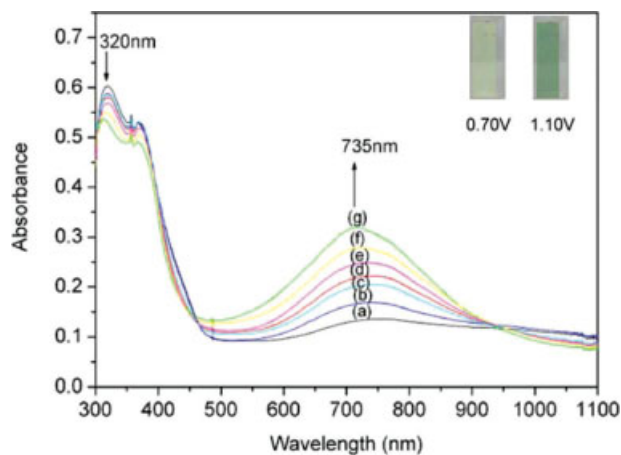
CONCLUSIONS

A series of new triphenylamine-based, high-performance polymers with strong fluorescence
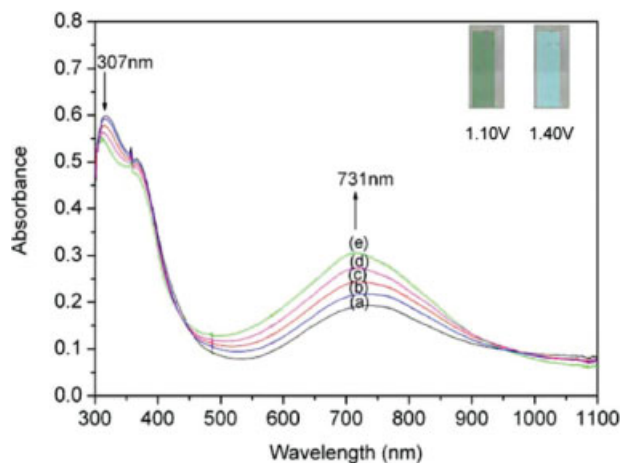

Figure 12. Electrochromic behavior of a polyamide **3e** thin film (in CH$_3$CN with 0.1 M TBAP as the supporting electrolyte) at (a) 0.00, (b) 0.55, (c) 0.58, (d) 0.62, (e) 0.65, (f) 0.68, and (g) 0.70 V.

Figure 13. Electrochromic behavior of a polyamide **3e** thin film (in CH$_3$CN with 0.1 M TBAP as the supporting electrolyte) at (a) 0.86, (b) 0.90, (c) 0.94, (d) 0.98, (e) 1.02, (f) 1.06, and (g) 1.10 V.

emissions in the blue region and high quantum yields up to 64% were successfully prepared from **2** with various diamines. The results presented here also demonstrated that incorporating a bulky, methyl-substituted triphenylamine group into the polymer backbone not only enhanced the processability of the rigid polymer backbone while maintaining good thermal stability but also provided stability for the electrochromic characteristics: the polymers changed in color from a pale yellowish neutral form to pale blue oxidized forms. Thus, these novel methyl-substituted triphenylamine polyamides have great potential as new blue-light-
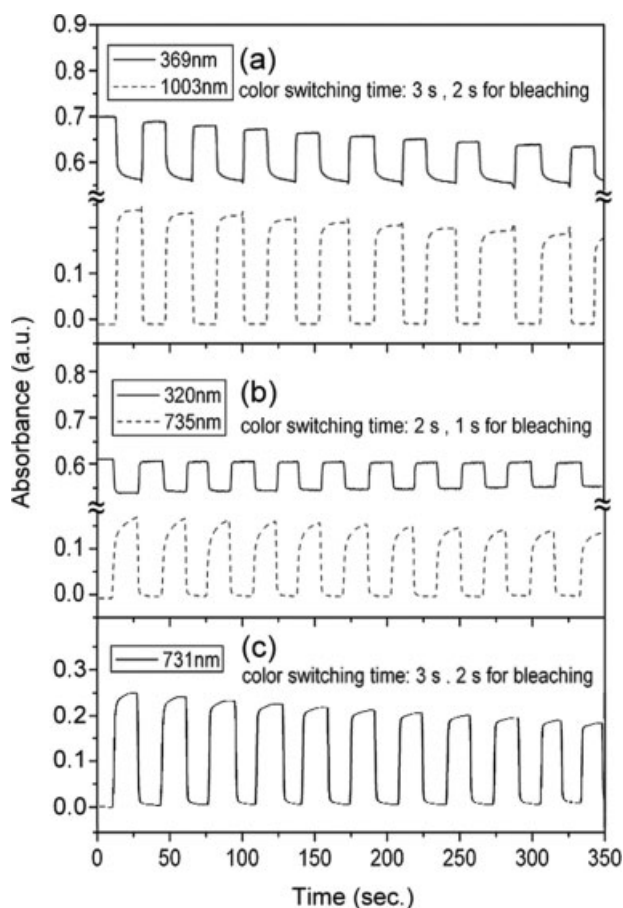

Figure 14. Electrochromic behavior of a polyamide **3e** thin film (in CH$_3$CN with 0.1 M TBAP as the supporting electrolyte) at (a) 1.19, (b) 1.22, (c) 1.26, (d) 1.30, (e) 1.33, (f) 1.36, and (g) 1.40 V.

Figure 15. Potential step absorptometry of polyamide **3e** (in CH$_3$CN with 0.1 M TBAP as the supporting electrolyte) by the application of a potential step: (a) 0 V $\leftrightarrow$ 0.70 V), (b) 0 V $\leftrightarrow$ 1.01 V), and (c) 0 V $\leftrightarrow$ 1.40 V.

emitting hole-transporting and electrochromic materials because of their proper HOMO values and excellent electrochemical and thermal stability.

REFERENCES AND NOTES

1. Tang, C.-W.; VanSlyke, S.-A. Appl Phys Lett 1987, 51, 913.
2. Tang, C.-W.; VanSlyke, S.-A.; Chen, C.-H. J Appl Phys 1989, 65, 3610.
3. Adachi, C.; Nagai, K.; Tamoto, N. Appl Phys Lett 1995, 66, 2679.
4. Shirota, Y. J. Mater Chem 2005, 15, 75.
5. Bellmann, E.; Shaheen, S.-E.; Grubbs, R. H.; Marder, S.-R.; Kippelen, B.; Peyghambarian, N. Chem Mater 1999, 11, 399.
6. Lu, J.-P.; Hlil, A.-R.; Sun, Y.; Hay, A.-S.; Maindron, T.; Dodelet, J.-P.; D'Iorio, M. Chem Mater 1999, 11, 2501.
7. Wang, X.-Q.; Chen, Z.-J.; Ogino, K.; Sato, H.; Strzelec, K.; Miyata, S.; Luo, Y.-J.; Tan, H.-M. Macromol Chem Phys 2002, 203, 739.
8. Fang, Q.; Yamamoto, T. Macromolecules 2004, 37, 5894.
9. Sun, M.-H.; Li, J.; Li, B.-S.; Fu, Y.-Q.; Bo, Z.-S. Macromolecules 2005, 38, 2651.
10. Liu, Y.-Q.; Liu, M.-S.; Li, X.-C.; Jen, A. K.-Y. Chem Mater 1998, 10, 3301.
11. Li, X.-C.; Liu, Y.-Q.; Liu, M.-S.; Jen, A. K.-Y. Chem Mater 1999, 11, 1568.
12. Redecker, M.; Bradley, D.-D.-C.; Inbasekaran, M.; Wu, W.-W.; Woo, E.-P. Adv Mater 1999, 11, 241.
13. Ego, C.; Grimsdale, A.-C.; Uckert, F.; Yu, G.; Srdanov, G.; Mullen, K. Adv Mater 2002, 14, 809.
14. Shu, C.-F.; Dodda, R.; Wu, F.-I.; Liu, M. S.; Jen, A. K.-Y. Macromolecules 2003, 36, 6698.
15. Wu, F.-I.; Shih, P.-I.; Shu, C.-F.; Tung, Y.-L.; Chi, Y. Macromolecules 2005, 38, 9028.
16. Li, H.; Hu, Y.; Zhang, Y.; Ma, D.; Wang, L.; Jing, X.; Wang, F. J Polym Sci Part A: Polym Chem 2004, 42, 3947.
17. Sung, H.-H.; Lin, H.-C. J Polym Sci Part A: Polym Chem 2005, 43, 2700.
18. Su, T.-X.; Hsiao, S.-H.; Liou, G.-S. J Polym Sci Part A: Polym Chem 2005, 43, 2085.
19. Liou, G.-S.; Yang, Y.-L.; Su, O. Y.-L. J Polym Sci Part A: Polym Chem 2006, 44, 2587.
20. Pu, Y.-J.; Soma, M.; Kido, J.; Nishide, H. Chem Mater 2001, 13, 3817.
21. Liang, F.-S.; Pu, Y.-J.; Kurata, T.; Kido, J.; Nishide, H. Polymer 2005, 46, 3767.
22. Liang, F.-S.; Kurata, T.; Nishide, H.; Kido, J. J Polym Sci Part A: Polym Chem 2005, 43, 5765.
23. Kim, Y.-H.; Zhao, Q.-H.; Kwon, S.-K. J Polym Sci Part A: Polym Chem 2006, 44, 172.
24. Miteva, T.; Meisel, A.; Knoll, W.; Nothofer, H.-G.; Scherf, U.; Muller, D.-C.; Meerholz, K.; Yasuda, A.; Neher, D. Adv Mater 2001, 13, 565.
25. Fu, Y.-Q.; Li, Y.; Li, J.; Yan, S.-K.; Bo, Z.-S. Macromolecules 2004, 37, 6395.
26. Son, J.-M.; Mori, T.; Ogino, K.; Sato, H.; Ito, Y. Macromolecules 1999, 32, 4849.
27. Ogino, K.; Kanegae, A.; Yamaguchi, R.; Sato, H.; Kurjata, J. Macromol Rapid Commun 1999, 20, 103.
28. Wu, A.; Kakimoto, M. Adv Mater 1994, 7, 812.
29. Nishikata, Y.; Fukui, S.; Kakimoto, M.; Imai, Y.; Nishiyama, K.; Fujihira, M. Thin Solid Films 1992, 210, 296.

30. Wu, A.; Jikei, M.; Kakimoto, M.; Imai, Y.; Ukishima, Y.-S.; Takahashi, Y. Chem Lett 1994, 2319.

31. Liou, G.-S.; Hsiao, S.-H.; Su, T.-X. J Polym Sci Part A: Polym Chem 2005, 43, 3245.

32. Cheng, S.-H.; Hsiao, S.-H.; Su, T.-H.; Liou, G.-S. Macromolecules 2005, 38, 307.

33. Liou, G.-S.; Hsiao, S.-H.; Su, T.-H. J Mater Chem 2005, 15, 1812.

34. Hsiao, S.-H.; Chen, C.-W.; Liou, G.-S. J Polym Sci Part A: Polym Chem 2004, 42, 3302.

35. Oishi, Y.; Mori, K.; Hirahara, H.; Fujimura, Y.; Miya, K. Japanese Patent 11–255723, 1999.

36. Tan, L.-S.; Srinivasan, K.-R.; Bai, S.-J. J Polym Sci Part A: Polym Chem 1997, 35, 1909.

37. Chen, Z.-K.; Huang, W.; Wang, L.-H.; Kang, E.-T.; Chen, B. J.; Lee, C. S.; Lee, S. T. Macromolecules 2000, 33, 9015.

38. Demas, J.-N.; Crosby, G.-A. J Phys Chem 1971, 75, 991.